Design of optical bandpass filters based on a two-material multilayer structure

B. A. Belyaev,[1,2,3,]* V. V. Tyurnev,[1,2] and V. F. Shabanov[1]

[1]*Kirensky Institute of Physics, Siberian Branch, Russian Academy of Sciences, Krasnoyarsk 660036, Russia*

[2]*Siberian Federal University, Krasnoyarsk 660041, Russia*

[3]*Reshetnev Siberian State Aerospace University, Krasnoyarsk 660014, Russia*

**Corresponding author: belyaev@iph.krasn.ru*

Received March 26, 2014; revised April 30, 2014; accepted May 10, 2014;
posted May 13, 2014 (Doc. ID 208890); published June 6, 2014

An easy method for designing filters with equalized passband ripples of a given magnitude is proposed. The filter, which is made of two dielectric materials, comprises coupled half-wavelength resonators and multilayer mirrors. The filter design begins with the synthesis of the multimaterial filter prototype whose mirrors consist of quarter-wavelength layers. Optimal refractive indices of the layers in the prototype are obtained by a special optimization based on universal rules. The thicknesses of the mirrors' layers in the final filter are computed using derived formulas. A design procedure example for silicon–air bandpass filters with a fractional bandwidth of 1% is described.

OCIS codes: (230.7408) Wavelength filtering devices; (310.6805) Theory and design; (310.4165) Multilayer design.
http://dx.doi.org/10.1364/OL.39.003512

Thin-film optical passband filters are used in optical communications, fluorescence microscopy, and astronomy. They are constructed using multilayer structures composed of alternating dielectric layers with high and low refractive indices. Two types of functional units can be singled out in such structures: resonators and multilayer mirrors.

The resonators usually consist of one layer with an optical thickness equal to half the wavelength of the center frequency of the filter passband or a multiple thereof. The resonators in a filter determine the center frequency and width of the passband.

The mirrors are situated between neighboring resonators or between the input/output resonator and the environment. Such mirrors usually consist of several layers, where the number of layers in the mirror depends on the passband width and may vary from one mirror to another. The optical thicknesses of the layers in the mirrors are usually equal to a quarter-wavelength. The mirrors are responsible for the stopband performance as well as for coupling the resonators. Therefore, the mirrors and resonators are equally responsible for the passband performance.

Multilayer filters usually have an unacceptably large transmittance ripple in the passband when their mirrors are made from two materials and all layers in the mirrors are quarter-wavelength [1]. In Ref. 1, "the dispersion of the equivalent admittance of the symmetrical period" in multilayer mirrors was said to be responsible for the large ripple. In reality, the cause is quite different. As is well known among microwave filter designers, this effect is actually caused by a mismatch between the resonators' couplings [2]. In the case of multilayer filters, that means there is a mismatch between the mirrors' reflectivities [3]. Therefore, accurate adjustment of multilayer filters requires fine optimization of the mirrors' reflectivities.

Such optimization was achieved in [3–6] by using multimaterial mirrors where the refractive indices of the materials were matched. However, precise matching in a real filter is not always possible because a material with the required refractive index may not exist.

Another approach to fine mirror adjustment in order to suppress the transmittance ripple was applied in [7–9]. This approach is based on the use of nonquarter-wave layers in the mirrors. Numerical optimization is needed for this approach, as well as numerous computations of target function sensitivities [7] or standing wave ratios [8,9].

In this Letter, we propose an easy and accurate method for the design of multilayer bandpass filters with a specified bandwidth and a specified magnitude of passband ripple. Here, the reflectivities of the multilayer mirrors are adjusted by the use of nonquarter-wave layers. The method may be realized without the use of any special software packages. High adjustment efficiency is achieved owing to the application of special rules.

The design method consists of two steps. The first step is the synthesis of the filter prototype with the required frequency response. All of the mirror layers in the prototype are quarter-wavelength. All high-refractive-index layers in all the mirrors have the same refractive index, n_H. All low-refractive-index layers in the ith mirror have the refractive index, n_i, where the refractive index varies depending on i. Thus, the refractive indices, n_i, are the only parameters of the prototype that are adjustable. Their optimal values can be easily obtained by numerical optimization if one applies the universal rules of filter optimization [3,10].

The second step is the replacement of every quarter-wavelength layer with refractive index, n_i, by the equivalent symmetric three-layer structure *H-L-H* with refractive indices, n_H, n_L, and n_H, where n_L is an arbitrary value that is less than any of the n_i values. Thus, the resultant filter is composed of only two materials with refractive indices, n_H and n_L. Its frequency response and that of the prototype coincide near the passband. One may read about the equivalent symmetric three-layer structures in Ref. 11.

We shall illustrate our design method by the following example. Let the center frequency, f_0, of the required filter passband be defined by the wavelength $\lambda = 3$ μm. The other parameters of the required passband are the

3 dB fractional bandwidth, $\Delta f/f_0 = 0.01$, and the reflection maximum, $S_{11\ \max} = -15$ dB, where S_{ij} are the scattering matrix elements [Fig. 1(a)]. Note that our design method is applicable for practically any center frequency, f_0, fractional bandwidth, $\Delta f/f_0$, and reflection maximum, $S_{11\ \max}$.

As a high-refractive-index material, we choose silicon ($n_H = 3.436$) and as a low-refractive-index material, we choose air ($n_L = 1$). Such a high n_H/n_L ratio allows the filter to have mirrors with a minimum number of dielectric layers.

We suppose the filter contains five air half-wavelength resonators. That means that the device has the frequency response of a fifth-order filter. Therefore, the reflection function, $S_{11}(f)$, has four maxima in the filter passband. Because $S_{11}(f)$ is a symmetric function relative to f_0, its maxima are symmetric too. Thus, the four reflection maxima have only two different amplitudes, yielding peaks of $S_{11\ \max 1}$, $S_{11\ \max 2}$, $S_{11\ \max 2}$, and $S_{11\ \max 1}$, ordered by increasing frequency [Fig. 1(b)].

Thus, the filter may be represented by the structure M_1-R-M_2-R-M_3-R-M_3-R-M_2-R-M_1, where R denotes the air half-wavelength resonator and M_i denotes the ith multilayer mirror ($i = 1, 2, 3$).

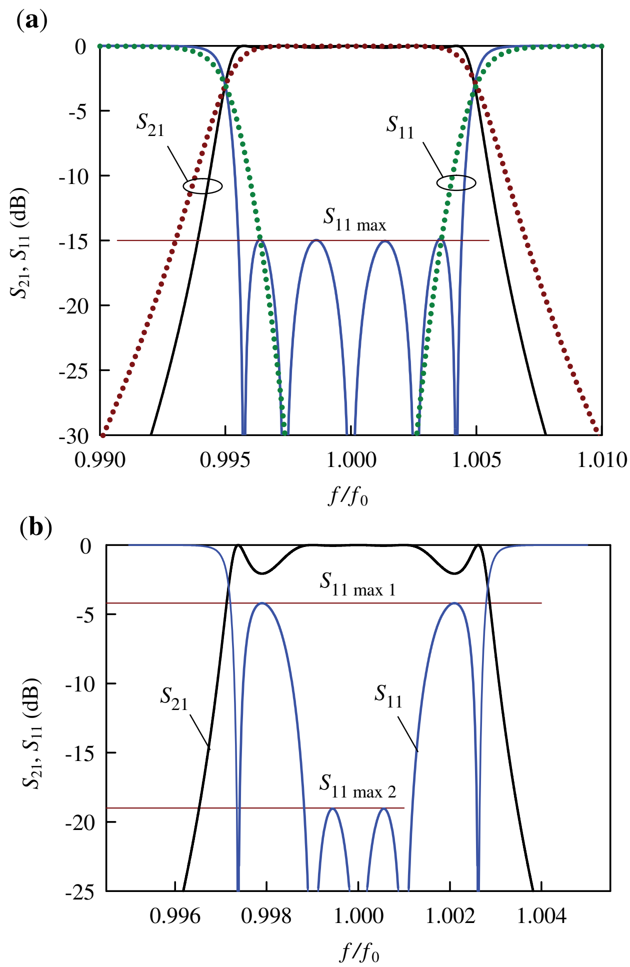

Fig. 1. Frequency response of the filter prototype (a) after and (b) before optimization. Here, S_{21} and S_{11} are reflection and transmission, respectively. Solid curves in (a) refer to the equalized ripple response (Chebyshev response) that is required and dotted curves refer to the flat-top response (Butterworth response) that is the alternative passband.

The goal of the prototype optimization is to find the optimal number of dielectric layers in the ith mirror together with the optimal value, n_i, that achieves the required passband.

We compute the frequency response of the filter using characteristic (i.e., *ABCD*) matrices [1,12,13]. Our direct numerical estimation says that the prototype can be made with 3 layers in mirror M_1, 7 layers in mirror M_2, and 7 layers in mirror M_3. Thus, the total number of layers in the entire prototype is 39.

We begin the prototype optimization with initial refractive index values, $n_1 = 1$, $n_2 = 1$, and $n_3 = 1$. Fig. 1(a) depicts the initial frequency response of the prototype, which shows that $S_{11\ \max 1} > S_{11\ \max 2}$. In order to turn this inequality into an equality, we should increase the difference, $n_2 - n_3$. In the current situation, that means only increasing n_2. In the case of $n_3 > 1$, we simultaneously increase n_2 and decrease n_3 by the same amount.

When the passband ripple has been equalized, we should adjust the passband width. In order to widen (narrow) the bandwidth, we should increase (decrease) the sum, $n_2 + n_3$. To maintain the previously set difference, $n_2 - n_3$, both n_2 and n_3 should be increased (decreased) by the same amount.

When the passband ripple and the bandwidth have been adjusted, we should adjust the quantity $S_{11\ \max} = (S_{11\ \max 1} + S_{11\ \max 2})/2$ to have the value -15 dB. In order to increase (decrease) the sum, $S_{11\ \max 1} + S_{11\ \max 2}$, we should increase (decrease) the refractive index, n_1.

Thus, there are three universal optimization rules for the fifth-order filter. The increase in the reflectivity of mirror M_2 and the simultaneous decrease in the reflectivity of mirror M_3 mainly result in a smaller difference, $S_{11\ \max 1} - S_{11\ \max 2}$. The increase in the reflectivity of mirror M_2 and simultaneous increase in the reflectivity of mirror M_3 mainly result in a narrower bandwidth, Δf. The increase in the reflectivity of mirror M_1 mainly results in a greater sum, $S_{11\ \max 1} + S_{11\ \max 2}$.

After completion of the rule optimization, the adjusted prototype obtains the final refractive index values, $n_1 = 1.5282$, $n_2 = 1.3035$, and $n_3 = 1.1934$. Fig. 1(a) shows the final frequency response of the prototype. It proves that the selectivity of the required prototype with the equalized ripple passband is higher than the selectivity of the alternative prototype with flat-top passband.

Now, we should substitute the equivalent symmetric three-layer structure H-L-H for every quarter-wavelength layer with refractive index n_i in the prototype. This structure is equivalent to the quarter-wavelength layer when it has the same characteristic matrix. Because the compared matrices are functions of frequency, the exact equality of the matrices may take place only at one frequency. We choose this frequency to be f_0. Thus, the equivalence of the three-layer structure for frequencies other than f_0 is only approximate.

Requiring that the diagonal elements of the compared matrices be equal yields the equation

$$(n_H^2 + n_L^2) \tan 2\theta_{Hi} \tan \theta_{Li} = 2 n_H n_L, \tag{1}$$

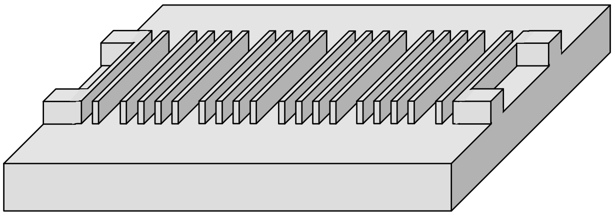

Fig. 2. Schematic sketch of the designed silicon–air filter.

where θ_{Hi} and θ_{Li} are the phase thicknesses of the high-refractive-index and low-refractive-index layers in the equivalent three-layer structure, respectively.

Requiring that the off-diagonal elements of the compared matrices be equal yields the equation

$$\sin 2\theta_{Hi} \cos \theta_{Li} + \left(\frac{n_L}{n_H} \cos^2 \theta_{Hi} - \frac{n_H}{n_L} \sin^2 \theta_{Hi} \right) \sin \theta_{Li} = \frac{n_i}{n_H}. \tag{2}$$

Here, we had in mind that the *H-L-H* structure is a reciprocal and symmetrical two-port network where the elements of the *ABCD* matrix are bounded by the constraints $AD - BC = 1$, $A = D$ [12].

Equations (1) and (2) have the solution

$$\tan^2 \theta_{Hi} = \frac{\sqrt{\begin{array}{l}(n_H^2 + n_L^2)^2 (n_H^2 - n_i^2)^2 \\ +4n_H^2 (n_H^4 - n_L^2 n_i^2)(n_i^2 - n_L^2)\end{array}} - (n_H^2 + n_L^2)(n_H^2 - n_i^2)}{2(n_H^4 - n_L^2 n_i^2)}, \tag{3}$$

$$\cot \theta_{Li} = \frac{n_H^2 + n_L^2}{2 n_H n_L} \tan(2\theta_{Hi}). \tag{4}$$

Equations (3) and (4) give the phase thicknesses of the high-refractive-index and low-refractive-index layers in the equivalent *H-L-H* structures of the mirrors, $\theta_{H1} = 0.10409\pi$, $\theta_{L1} = 0.19441\pi$, $\theta_{H2} = 0.07643\pi$, $\theta_{L2} = 0.25473\pi$, $\theta_{H3} = 0.05993\pi$, and $\theta_{L3} = 0.29796\pi$.

The resultant high-refractive-index layer in every mirror is composed of the initial quarter-wavelength layer and one or two additional layers of the adjacent equivalent *H-L-H* structures. Therefore, the outer high-refractive-index layers in mirror M_i impart a phase shift of $\pi/2 + \theta_{Hi}$, and the inner layers also produce a phase shift of $\pi/2 + 2\theta_{Hi}$. The low-refractive-index layers in mirror M_i have a phase thickness of θ_{Li}.

That means that the physical thicknesses of the high-refractive-index layers are the following: 264 nm for the layers in mirror M_1; 252 and 285 nm for the outer and inner layers in mirror M_2, respectively; and 244 and 271 nm for the outer and inner layers in mirror M_3. The thicknesses of the low-refractive-index layers are as follows: 292 nm in mirror M_1, 382 nm in mirror M_2, and 447 nm in mirror M_3.

Figure 2 shows a possible example of an implementation of the designed silicon–air filter. The fabrication of a similar design using wet etching as well as e-beam lithography and inductively coupled plasma etching was described in Refs. 6 and 14.

Figure 3 shows the computed frequency responses of the designed filter and its prototype. Both the responses have the same passband. However, their lower and upper stopbands are somewhat different far from the center frequency, f_0, where the equivalence of the *H-L-H* structures, substituting for the quarter-wavelength layers in the mirrors, decays.

Note that the proposed design method may also be applied for the filters that are fabricated by multilayer deposition on a substrate [15,16]. In this case, one should first design the temporary filter without the substrate. Then, the substrate should be integrated with one of the outer multilayer mirrors of the temporary filter. Once the substrate is included, the mirror to which it is in contact should be reoptimized.

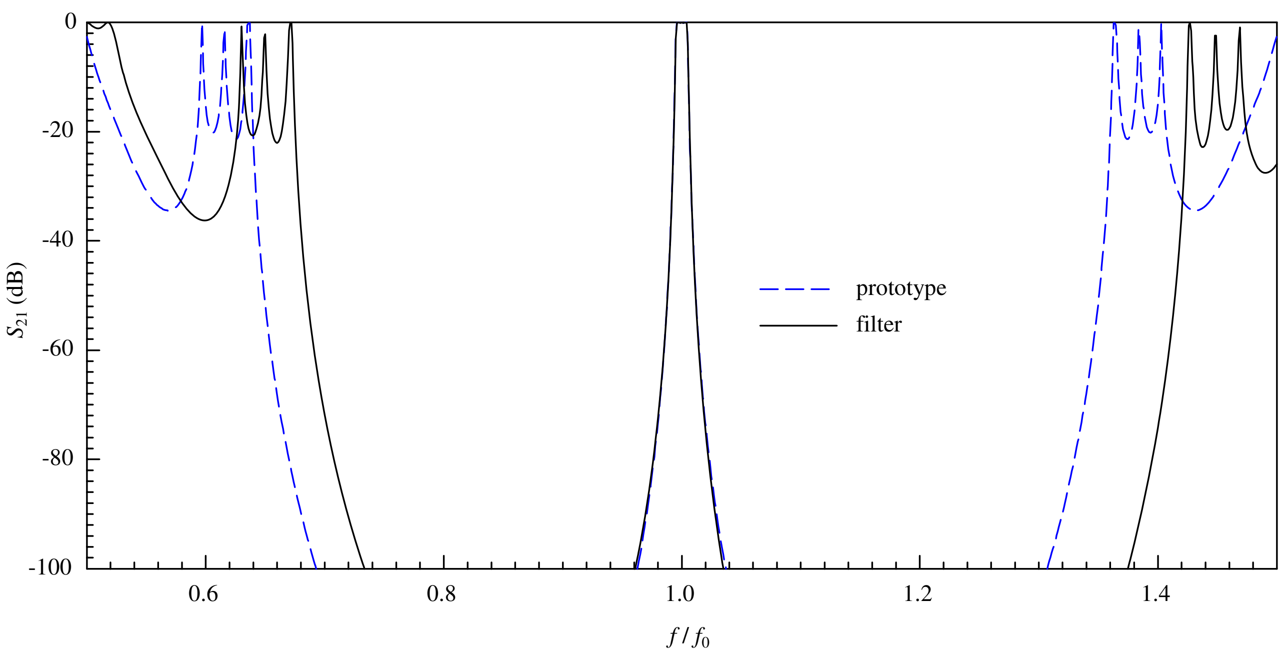

Fig. 3. Computed frequency responses of the designed filter and its prototype.

The authors acknowledge support in part by the Siberian Branch of the Russian Academy of Sciences under Integration Project No. 109.

References

1. H. A. Macleod, *Thin-Film Optical Filters* (CRC Press, 2010).
2. G. L. Matthaei, L. Young, and E. M. Jones, *Microwave Filters, Impedance-Matching Networks, and Coupling Structures* (Artech House, 1980).
3. B. A. Belyaev, V. V. Tyurnev, and V. F. Shabanov, Dokl. Phys. **59**, 73 (2014).
4. S. Dasgupta, S. Mandal, and C. Bose, *International Conference on Communications, Devices and Intelligent Systems* (IEEE, 2012), pp. 184–187.
5. S. Yu and J. Zhang, *Asia Communications and Photonics Conference and Exhibition*, Technical Digest (CD) (Optical Society of America, 2009), Vol. **7630**, paper TuV5.
6. A. Baldycheva, V. A. Tolmachev, T. S. Perova, Y. A. Zharova, E. V. Astrova, and K. Berwick, Opt. Lett. **36**, 1854 (2011).
7. P. G. Verly, Proc. SPIE **5250**, 378 (2004).
8. P. Baumeister, Opt. Express **9**, 652 (2001).
9. P. Baumeister, Appl. Opt. **42**, 2407 (2003).
10. B. A. Belyaev and V. V. Tyurnev, *16th International Crimean Conference Microwave and Telecommunication Technology* (CriMiCO, 2006) Vol. **2**, pp. 517–519.
11. A. Thelen, *Design of Optical Interference Coatings* (McGraw Hill, 1989), Section 3.1.
12. K. C. Gupta, R. Garg, and R. Chadha, *Computer-Aided Design of Microwave Circuits* (Artech House, 1981).
13. B. A. Belyaev, V. V. Tyurnev, and V. F. Shabanov, Russ. Phys. J. **56**, 1378 (2014).
14. W. Jia, J. Deng, B. P. L. Reid, X. Wang, C. C. S. Chan, H. Wu, X. Li, R. A. Taylor, and A. J. Danner, Photo. Nano. Fund. Appl. **10**, 447 (2012).
15. N. Kaizer, Appl. Opt. **41**, 3053 (2002).
16. B. T. Sullivan, G. A. Clarke, T. Akiyama, N. Osborne, M. Ranger, J. A. Dobrowolski, L. Howe, A. Matsumoto, Y. Song, and K. Kikuchi, Appl. Opt. **39**, 157 (2000).